Protein/Lipid Interaction in the Bacterial Photosynthetic Reaction Center: Phosphatidylcholine and Phosphatidylglycerol Modify the Free Energy Levels of the Quinones †

ARTICLE *in* BIOCHEMISTRY · NOVEMBER 2004

Impact Factor: 3.02 · DOI: 10.1021/bi0489356 · Source: PubMed

9 AUTHORS, INCLUDING:

Francesco Milano
Italian National Research Council
71 PUBLICATIONS **390** CITATIONS
SEE PROFILE

Marta Dorogi Dr.
Hungarian Academy of Sciences
14 PUBLICATIONS **158** CITATIONS
SEE PROFILE

Angela Agostiano
Università degli Studi di Bari Aldo Moro
358 PUBLICATIONS **4,074** CITATIONS
SEE PROFILE

Massimo Trotta
Italian National Research Council
117 PUBLICATIONS **550** CITATIONS
SEE PROFILE

Protein/Lipid Interaction in the Bacterial Photosynthetic Reaction Center: Phosphatidylcholine and Phosphatidylglycerol Modify the Free Energy Levels of the Quinones†

László Nagy,‡ Francesco Milano,§ Márta Dorogi,‡ Angela Agostiano,|| Gábor Laczkó,‡ Kornélia Szebényi,‡ György Váró,⊥ Massimo Trotta,§ and Péter Maróti*,‡

Department of Biophysics, University of Szeged, Szeged, Hungary, CNR, Istituto per i Processi Chimico-Fisici, Sezione di Bari, and Department of Chemistry, University of Bari, Bari, Italy, and Institute of Biophysics, Biological Research Center, Szeged, Hungary

Received May 25, 2004; Revised Manuscript Received August 5, 2004

ABSTRACT: The role of characteristic phospholipids of native membranes, phosphatidylcholine (PC), phosphatidylglycerol (PG), and cardiolipin (CL), was studied in the energetics of the acceptor quinone side in photosynthetic reaction centers of *Rhodobacter sphaeroides*. The rates of the first, $k_{AB}(1)$, and the second, $k_{AB}(2)$, electron transfer and that of the charge recombination, k_{BP}, the free energy levels of $Q_A^-Q_B$ and $Q_AQ_B^-$ states, and the changes of charge compensating protein relaxation were determined in RCs incorporated into artificial lipid bilayer membranes. In RCs embedded in the PC vesicle, $k_{AB}(1)$ and $k_{AB}(2)$ increased (from 3100 to 4100 s^{-1} and from 740 to 3300 s^{-1}, respectively) and k_{BP} decreased (from 0.77 to 0.39 s^{-1}) compared to those measured in detergent at pH 7. In PG, $k_{AB}(1)$ and k_{BP} decreased (to values of 710 and 0.26 s^{-1}, respectively), while $k_{AB}(2)$ increased to 1506 s^{-1} at pH 7. The free energy between the $Q_A^-Q_B$ and $Q_AQ_B^-$ states decreased in PC and PG ($\Delta G°_{Q_A^-Q_B \rightarrow Q_AQ_B^-} = -76.9$ and -88.5 meV, respectively) compared to that measured in detergent (-61.8 meV). The changes of the Q_A/Q_A^- redox potential measured by delayed luminescence showed (1) a differential effect of lipids whether RC incorporated in micelles or vesicles, (2) an altered binding interaction between anionic lipids and RC, (3) a direct influence of PC and PG on the free energy levels of the primary and secondary quinones probably through the intraprotein hydrogen-bonding network, and (4) a larger increase of the Q_A/Q_A^- free energy in PG than in PC both in detergent micelles and in single-component vesicles. On the basis of recent structural data, implications of the binding properties of phospholipids to RC and possible interactions between lipids and electron transfer components will be discussed.

The primary processes of photosynthesis take place in a specialized pigment−protein system called the photosynthetic reaction center (RC)[1] embedded in the thylakoid membranes of chloroplast and in the intracytoplasmic membrane systems (ICM) of cyanobacteria and photosynthetic bacteria. The capture of light energy by bacteriochlorophylls in photosynthetic bacteria is followed by separation of positive and negative charges as P^+BPheo^- and then $P^+Q_A^-$. Here P^+ is the oxidized primary donor, a specialized bacteriochlorophyll dimer, BPheo is the first electron acceptor, a monomer bacteriopheophytin, and Q_A^- is the reduced quinone-type primary electron acceptor. The separated charges are further stabilized in the form of the $P^+Q_B^-$ redox state, where Q_B^- is the reduced secondary quinone (for reviews, see, e.g., refs *1*−*5*). Although the quantum efficiency of the primary charge separation is close to 1 in the RC (*6*), the physical parameters of the electron transport depend on the type of the RC and environmental factors. From this point of view, the membrane environment is of special interest, since one of the main goals of RC studies is to understand its function in vivo.

The kinetics and thermodynamics of the electron transfer reactions in RCs are mainly studied in detergent micelles, because the membrane lipids are replaced by detergent molecules during the purification procedure. The role played by the detergent goes further than solubilization of the protein. There are indications that the surfactant environment of the RCs in the ordered (boundary) region influences the electronic structure of the cofactors (*7*, *8*), consequently the electron transfer kinetics, and interacts with the channel in which UQ_{10} is taken up or released (*9*). The strong binding

† This work was supported by grants from the Hungarian Science Foundation (OTKA, T034788 and T42680), the MTA/CNR cooperation program, and Italian government grants Meccanismi Molecolari della Fotosintesi (FIRB-MIUR) and Cofin−MIUR 2002.

* To whom correspondence should be addressed. Phone: 36-62-544-120. Fax: 36-62-544-121. E-mail: pmaroti@physx.u-szeged.hu.
‡ University of Szeged.
§ Istituto per i Processi Chimico-Fisici.
|| University of Bari.
⊥ Biological Research Center.

[1] Abbreviations: BChl, bacteriochlorophyll; *Blc*., *Blastochloris*; BPheo, bacteriopheophytin; CL, cardiolipin; DGDG, digalactosyldiacylglycerol; cyt c^{2+}, reduced cytochrome; DL, delayed luminescence; LDAO, *N*,*N*-dimethyldodecylamine *N*-oxide; MGDG, monogalactosyldiacylglycerol; P, primary donor; PC, phosphatidylcholine; PE, phosphatidylethanolamine; PG, phosphatidylglycerol; Q, fully oxidized ubiquinone-10; UQ_{10}, 2,3-dimethoxy-5-methyl-6-decaisoprenol-*p*-benzoquinone; Q_A, primary quinone acceptor; Q_B, secondary quinone acceptor; *Rb*., *Rhodobacter*; RC, reaction center; TX, Triton X-100.

10.1021/bi0489356 CCC: $27.50
Published on Web 09/21/2004

of the detergents to the RCs is verified by the cocrystallization of these molecules with the RCs (*10*−*14*). However, there are more and more indications that the kinetics and thermodynamics of the electron transfer reactions in RCs have different features in chromatophores, which resemble the conditions in vivo. The first (*15*) and the second (*16*) electron transfer and the $P^+Q_A^- \rightarrow PQ_A$ charge recombination (*17*) have been found to be significantly faster in the native membrane than in detergent (*18*, *19*). The free energy gap associated with the $Q_A^-Q_B \rightarrow Q_AQ_B^-$ electron transfer increases in the sequence of detergent → liposome → chromatophore system (*18*).

The phospholipid composition of the chromatophore membrane of *Rhodobacter sphaeroides* is not unique. Grown under phototropic high light conditions, the ICM consists of four major phospholipid components: phosphatidylcholine (PC), phosphatidylethanolamine (PE), cardiolipin (CL), and phosphatidylglycerol (PG) (*18*, *20*, *21*). Elevated levels of PG in *Rhodobacter capsulatus* (*22*) and CL in *Rb. sphaeroides* (*23*) in cells growing under photoheterotrophic conditions have also been reported. PG is the only lipid common to *Rb. sphaeroides*, *Rb. capsulatus*, *Rhodopseudomonas palustris*, *Rhodopseudomonas gelatinosa*, *Rhodospirillum rubrum*, green bacteria, and chloroplasts (*21*).

The lipid environment provides the structural environment for the RC and regulates its function (*19*, *24*−*27*). Four aspects of the interaction should be stressed. (i) The structural flexibility of the proteins is larger in the photosynthetic membrane than in the artificial detergent system, indicating that the degree of freedom of the movements of amino acid side chains is larger in the membrane (*18*). (ii) The response of biological (also photosynthetic) membranes to various extra- and intracellular signals leads to changes in the concentration, structure, and chemical composition of the proteins and lipids. To achieve this function, the cells have to keep close to the limit of the bilayer stability (*28*) that can be controlled by the appropriate incorporation of bilayer-forming (e.g., DGDG, PC, PG) and nonbilayer-forming (e.g., MGDG, PE) lipids. (iii) There are inherent components of the photosynthetic membranes that play a regulatory role in the photochemical energy conversion. Most typical examples are the ubiquinones, which are redox-active cofactors of the electron transport of RC in the purple bacterial membranes and plastoquinones in thylakoids of oxygen-evolving systems (*2*, *5*). (iv) Specific molecules (e.g., lipids) bind to specific sites of the RCs; thus they modify the physical parameters of the charge stabilization, but they are not involved inherently in the transient redox processes. The atomic resolution of RC crystals derived from *Blastochloris viridis* (formerly *Rhodopseudomonas viridis*) revealed that LDAO detergent molecules and SO_4^{2-} ions were bound to specific surface groups of the protein (*29*). It was demonstrated that the detergent molecules in isolated RC determined the accessibility of quinones to the Q_B binding site (*30*). Association of key phospholipids [CL (*11*, *31*, *32*), PC (*32*), and PE (*10*, *33*)] to the bacterial RC crystals was also suggested. Specific binding of PG to the D1 protein (*34*) and to the specific functional site of PS II in vivo was also shown (*35*−*37*).

Various stress conditions, including high light stress, have been suggested to be in connection with the role of lipids (*38*). One example is PG, which is essential for cell growth and for normal function of the electron transport system in PS II (*35*). In vivo functional assays demonstrated that the primary target site of PG was Q_B rather than Q_A, and PG should have been an indispensable component of the PS II complex to maintain the structural integrity of the Q_B-binding site (*37*).

Earlier studies implicated that the $Q_A^-Q_B$ to $Q_AQ_B^-$ electron transfer was dependent on the orientation of the partners, more precisely on the position of Q_B within the protein ("conformational gating"; *39*). However, this concept in its simple form became controversial recently (*40*, *41*). The analysis of mutants where the Pro L209 was replaced by different amino acids, especially by Tyr (*42*), indicated that the structure of the Q_B site was dependent not only on the redox state of Q_B but also on the physicochemical properties of the microenvironment of the Q_B site.

In this work we offer direct evidence for the role of characteristic native phospholipids of the prokaryotic and eucaryotic membranes, phosphatidylcholine (PC), phosphatidylglycerol (PG), and cardiolipin (CL), in charge stabilization in the RC isolated from purple bacteria. Light-induced absorption changes and delayed fluorescence measurements provided several new previously unobserved features due to different phospholipid environments in liposomes. The new kinetic and energetic observations are assigned to special modes of RC−lipid interactions. Implications for the RC in the native membrane will be discussed.

MATERIALS AND METHODS

Cell Cultivation and RC Preparations. Carotenoid-less *Rb. sphaeroides* R-26 cells were grown photoheterotrophically under anaerobic conditions in medium supplemented with potassium succinate (*43*). Chromatophores and RCs were prepared as described earlier (*44*). RCs were solubilized by LDAO (*N*,*N*-dimethyldodecylamine *N*-oxide; Fluka) and purified by ammonium sulfate precipitation followed by DEAE-Sephacel (Sigma) anion-exchange chromatography. The fractions of OD_{280}/OD_{803} ratio between 1.27 and 1.50 were collected and used for further experiments.

Liposome Preparations. Unilamellar RC/phospholipid vesicles were made by the micelle-to-vesicle transition method as described recently (*45*, *46*). The required amount of lipids (PC, 1,2-diacyl-*sn*-glycero-3-phosphocholine; PG, 1,2-diacyl-*sn*-glycero-3-phospho-(1-*rac*-glycerol); CL, diphosphatidylglycerol, sodium salt from bovine heart; all from Sigma) and quinone, UQ_{10} (2,3-dimethoxy-5-methyl-6-decaisoprenol-*p*-benzoquinone; Sigma), were dissolved in chloroform and dried on the surface of a conical Eppendorf tube, and the mixed micelles with phosphate buffer containing sodium cholate detergent were prepared by sonication. In some experiments, to block the Q_B site, the chloroform solution of different lipids was added with inhibitor terbutryn. After the addition of the RCs, the detergent was removed by Sephadex G-50 gel filtration.

Kinetic Absorption Spectrophotometry. Flash-induced absorption changes were measured routinely by a single-beam kinetic spectrophotometer of local design (*44*, *47*, *48*). The P/P^+ and Q/Q^- redox changes of the primary bacteriochlorophyll dimer and the quinones at the acceptor complex (*18*, *44*) and the electrochromic response of the absorption of bacteriopheophytins to the $Q_A^-Q_B$ and $Q_AQ_B^-$ states (*15*)

were detected at 603, 450, and 771 nm, respectively. The apparent one-electron equilibrium constant in the acceptor quinone complex, $K_{AB} = [Q_AQ_B^-]/[Q_A^-Q_B]$, was determined from the rate constants of the fast (k_f) and slow (k_s) components of the $P^+(Q_AQ_B)^- \rightarrow PQ_AQ_B$ charge recombination in the dark: $K_{AB} = k_f/k_s - 1$. The free energy gap between $Q_A^-Q_B$ and $Q_AQ_B^-$ states is $\Delta G°_{AB} = -k_BT \ln K_{AB}$, where k_B and T are the Boltzmann constant and the absolute temperature, respectively (*49*, *50*).

The quinone binding equilibrium constant of the Q_B site, $K_q = [Q_AQ_B]/[Q_A...] = [Q_A^-Q_B]/[Q_A^-...]$, was obtained from the model of the oscillation pattern of the semiquinone signal measured at 450 nm upon subsequent flash excitation of the RC (*18*, *47*, *51*). Here $[Q_A...]$ and $[Q_A^-...]$ denote the concentrations of the RC in oxidized and reduced states of the primary quinone, respectively. These species are able to bind quinone to the temporarily empty Q_B site.

Delayed Luminescence Measurements. Delayed luminescence was measured by a home-built fluorometer as described earlier (*52*). The sample was excited by a Q-switched Nd:YAG laser (Qantel YG 781-10; 532 nm, 100 mJ, 5 ns). The delayed luminescence was focused onto a photocathode of the red sensitive photomultiplier (Hamamatsu R-3310-03), which was thermostated at −30 °C (Photocool PC 410CE). A total of 256 traces (taken with 0.25 Hz repetition rate) were averaged by a digital oscilloscope (Philips PM 3350A), then stored, and analyzed by a personal computer. The $\Delta G°_{P*\rightarrow Q_A^-}$ standard free energy change of the $P*/P^+ \rightarrow Q_A/Q_A^-$ electron transport was calculated from the ratio of the total energies emitted in the form of the prompt, $\int F_p(t)\,dt$, and delayed, $\int F_d(t)\,dt$, fluorescence (*52*):

$$\Delta G°_{P*\rightarrow Q_A^-} = k_BT \ln \frac{k_d\Phi_f}{k_f\Phi_p} \frac{\int F_p(t)\,dt}{\int F_d(t)\,dt} \qquad (1)$$

where k_f ($=8 \times 10^7\ s^{-1}$) is the radiative rate constant for the RC dimer, Φ_p is the quantum yield of the charge separation [≈1.0 (*6*)], k_d is the rate constant of the decay of the $P^+Q_A^-$ charge pair, and Φ_f ($=4.0 \times 10^{-4}$) is the yield of the prompt fluorescence of the P*.

RESULTS

Light-induced electron transfer characteristics were measured and compared in RCs embedded in vesicles constructed from different phospholipids to get a closer look at the RC/lipid interaction. The applied assays are suited to follow the kinetics of various electron transfer reactions and the changes in the energetics of the acceptor quinone system.

$Q_A^-Q_B \rightarrow Q_AQ_B^-$ Electron Transfer. The light-induced difference absorption spectra of $PQ_A/P^+Q_A^-$ and $PQ_B/P^+Q_B^-$ have characteristic isosbestic points around 745 nm for Q_B^- and 752.5 nm for Q_A^- and minimum and maximum at lower and higher wavelengths, respectively [data not shown (*16*)]. Figure 1 shows the kinetics of the flash-induced absorption change (at 771 nm) of the RCs incorporated into LDAO detergent micelles and PC and PG liposomes. At this wavelength a shift in the electrochromic response of the BPheo absorption due to the electric field perturbation around the chromophore associated with the charge-compensating protein relaxation events can be measured (*15*). The time window is very wide (it covers 6 orders of magnitude); thus both the $P^+Q_A^-Q_B \rightarrow P^+Q_AQ_B^-$ electron transfer and the accompanied reactions (fast phase) and the $P^+(Q_AQ_B)^- \rightarrow PQ_AQ_B$ charge recombination (slow phase) can be followed in one plot of the logarithmic time scale. The kinetic parameters (amplitudes and rate constants) obtained from multiexponential decomposition are summarized in Table 1. The time resolution was limited to a few tens of microseconds under our conditions.

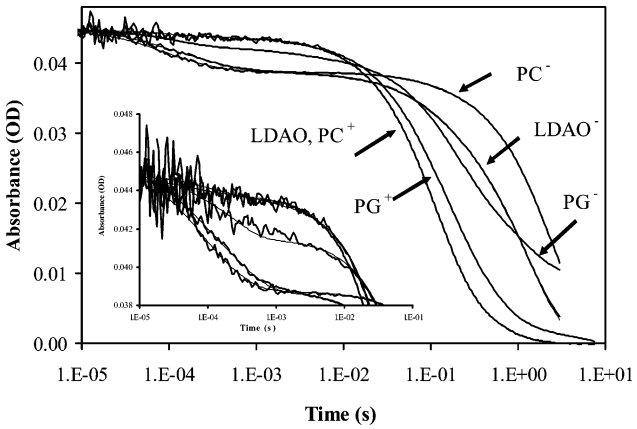

FIGURE 1: Absorption change of RCs of *Rb. sphaeroides* R-26 after single saturating laser flash excitation measured at 771 nm. The RCs were incorporated into LDAO detergent and PC or PG liposomes as indicated. For inhibition of the interquinone electron transfer, 100 μM terbutryn was added to the LDAO and PC and 400 μM to the PG samples. (+) and (−) indicate the presence or the absence of the terbutryn, respectively. Thin solid lines are the best fits with the parameters in Table 1. Inset: Absorption change in the submillisecond to millisecond time scale. Conditions: excitation at 597 nm; 3 μM RC, 10 mM Tris, 100 mM NaCl, and 0.01% LDAO, pH 8.0 (LDAO), and 5 mM phosphate and 5 mM KCl, pH 6.8 (PC and PG liposomes).

The rates of the fastest phase, $k_{AB}(1)_{fast}$, for the LDAO, PC, and PG samples were 16 800, 15 500, and 16 700 s^{-1}, respectively, the values of which were comparable to those reported in the literature for samples where the quinones were first depleted and then reconstituted (*15*). A slower component of a few hundreds of microsecond related to the interquinone electron transfer was also resolved [$k_{AB}(1)_{slow}$]. This phase is characteristic of the charge relaxation within the protein induced by the charge separation and the forward electron transfer (*15*, *53*) and may reflect the protonation of the characteristic amino acid residues of the protein. It can limit kinetically the overall electron transport between Q_A^- and Q_B. Our measurements clearly indicate that both the PC and PG lipid environments modify both the size (amplitude) and the rate of the charge relaxation processes of the protein. In PC, the rate of the overall electron transport increased by a factor of 1.3 compared to that of the LDAO (3100 s^{-1} increased to 4100 s^{-1}). This is in good agreement with the value reported by Taly et al. (*19*). In PG, however, we measured a rate constant of 710 s^{-1}, which is significantly (4.4 times) smaller than that in LDAO.

Both the interquinone electron transfer and the charge recombination were sensitive to the Q_B site inhibitor, terbutryn, and the effect was different in different environments (Figure 1). The electron transfer between Q_A and Q_B in PC and LDAO was almost completely blocked by 100 μM inhibitor. In contrast, in PG a large fraction (about 40%) of the electron transfer was obtained even in the presence of a very high concentration (400 μM) of terbutryn.

Table 1: Decomposition of Absorption Change Kinetics at 771 nm Associated to the $P^+Q_A^-Q_B \rightarrow P^+Q_AQ_B^-$ (First Electron Transfer) and $P^+(Q_AQ_B)^- \rightarrow P(Q_AQ_B)$ Charge Recombination (Figure 1) and at 450 nm (in the Presence of Cytochrome Donor) Attributed to $PQ_A^-Q_B^- \rightarrow PQ_AQ_B^{2-}$ Second Electron Transfer (Not Shown)[a]

	$(Q_A^-Q_B \rightarrow Q_AQ_B^-)_1$		$(Q_A^-Q_B \rightarrow Q_AQ_B^-)_2$		$(Q_A^-Q_B^- \rightarrow Q_AQ_B^{2-})$	$P^+Q_A^- \rightarrow PQ_A$		$P^+(Q_AQ_B)^- \rightarrow P(Q_AQ_B)$	
	A (%)	$k_{AB}(1)_{fast}$ (s^{-1})	A (%)	$k_{AB}(1)_{slow}$ (s^{-1})	$k_{AB}(2)$ (s^{-1})	A (%)	k_{AP} (s^{-1})	A (%)	k_{BP} (s^{-1})
LDAO	5.7	16 800	8.4	3100	740	11.9	9.3	73.9	0.77
PC	7.6	15 500	6.2	4100	3300	1.7	9.3	84.4	0.39
PG	6.0	16 700	3.4	710	1500	41.4	4.9	49.2	0.26

[a] RCs of *Rb. sphaeroides* R-26 were incorporated into PC or PG vesicles or LDAO detergent micelles. A (%) and k are the relative amplitude (in the percentage of that of the total signal) and the rate constants of the components, respectively. The maximum error of the measurement was 13%.

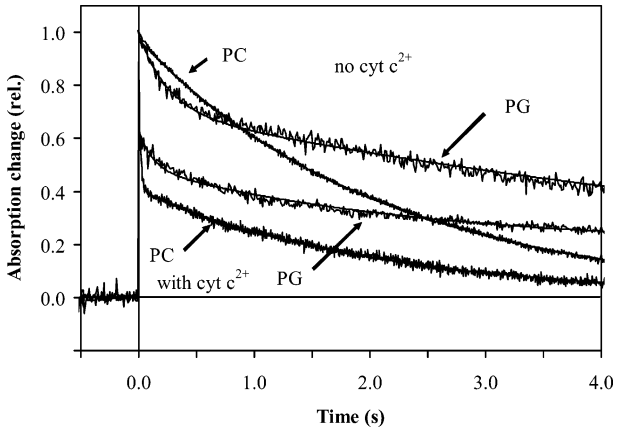

FIGURE 2: Kinetics of the flash-induced absorption change of RCs of *Rb. sphaeroides* R-26 detected at 603 nm in the presence (40 μM) or in the absence of reduced cytochrome (inverted direction). The RCs were incorporated into PC and PG liposomes. Solid lines are the best fits with the values listed in Table 2. Conditions are the same as in Figure 1.

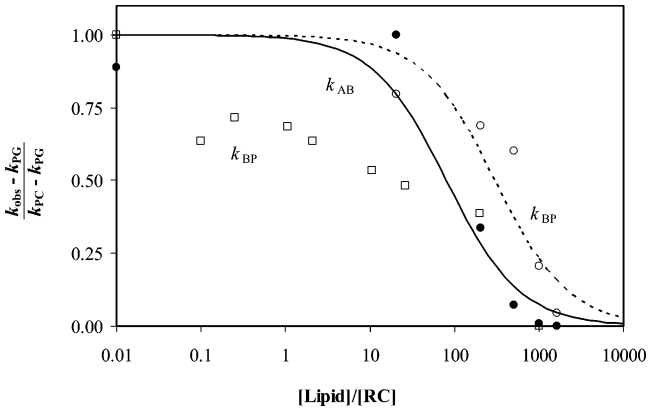

FIGURE 3: Rate constants of the $P^+Q_A^-Q_B \rightarrow P^+Q_AQ_B^-$ interquinone electron transfer [●, $k_{AB}(1)_{slow}$] and the $P^+(Q_AQ_B)^- \rightarrow P(Q_AQ_B)$ charge recombination [○ (PG) and □ (CL), k_{BP}] of RCs reconstituted in PC vesicles as a function of added PG (●, ○) or CL (□). The observed rate constants (k_{obs}) were normalized to those measured in pure PC (k_{PC}) and PG (k_{PG}) vesicles. Lines for the PG samples were calculated from the Michaelis−Menten equation [$(k_{obs} - k_{PG})/(k_{PC} - k_{PG}) = 1 - 1/(1 + K_{PG}/[PG])$; see explanation in the text]. Conditions are the same as in Figure 1.

$P^+(Q_AQ_B)^- \rightarrow PQ_AQ_B$ Charge Recombination. The kinetic traces detected at 603 nm showed clear biphasicity on the time scale of seconds [see Figure 2 for PC and PG liposomes and Nagy et al. (*18*) for detergent]. In detergent and PC liposomes, the rate constant of the fast component (attributed to $P^+Q_A^- \rightarrow PQ_A$) was $k_{AP} \sim 10\ s^{-1}$. In PG/RC samples, the fast component was measured in two different ways. (1) The Q_B site inhibitor, terbutryn, was added to the liposome during the preparation. (2) The quinone at the Q_B site was removed (up to 95% efficiency) by a standard procedure (*54*). Surprisingly, no complete block was observed after addition of a large excess (about 400 μM) of terbutryn in the PG/RC samples. The rate constant of the fast phase of the charge recombination was $k_{AP} = 6.3\ s^{-1}$ for the terbutryn-treated, but originally Q_B active sample, and about 30−40% slow phase was still observed. For the Q_B-depleted samples (5% Q_B was determined after the Q_B depletion procedure in detergent) a single exponential component with the rate constant $k_{AP} = 7.6-7.1\ s^{-1}$ was measured in the herbicide-treated sample (in detergent $k_{AP} = 10\ s^{-1}$; data not shown). To our surprise, the fast phase did not disappear in the presence of a large excess of quinone (UQ_{10}:RC = 20:1) but remained a fraction of 30−40% of the total amplitude with a somewhat smaller rate constant ($k_{AP} = 5.0\ s^{-1}$) (Figure 2).

The rate constant of the slow phase is indicative of the apparent electron equilibrium constant, K_{AB}, between the $Q_A^-Q_B$ and $Q_AQ_B^-$ states and can be used for determination of the $\Delta G°_{Q_A^-Q_B \rightarrow Q_AQ_B^-}$ free energy change of the $P^+Q_A^-Q_B \rightarrow P^+Q_AQ_B^-$ electron transfer (*49*, *50*). The rate constants of the slow phase in LDAO, PC, and PG were $k_{BP} = 0.83\ s^{-1}$, $k_{BP} = 0.38\ s^{-1}$, and $k_{BP} = 0.13\ s^{-1}$, respectively. These values correspond to about −62, −77, and −89 meV free energy changes in LDAO, PC, and PG, respectively.

The rate constants of the interquinone electron transfer and the charge recombination can be used to monitor the affinity of different lipids to the RC. The RC protein was embedded in PC vesicles in which different amounts of PG or CL phospholipids were also incorporated, and the rate constants of the electron transfer in the liposome of mixed lipids were measured (Figure 3). Starting from the pure PC vesicle, the rate of the slow phase of the $Q_A^-Q_B \rightarrow Q_AQ_B^-$ electron transfer, $k_{AB}(1)_{slow}$, decreased gradually with increasing amount of PG in the vesicle and reached a minimum level observed in pure PG (Figure 3). About 80 PG/RC can be determined for the 50% change in the PG/PC/RC vesicles. Similarly to the electrochromic shift experiments, k_{BP} of the $P^+(Q_AQ_B)^- \rightarrow PQ_AQ_B$ charge recombination was also determined in PG/PC/RC mixed liposomes where the PG content changed monotonically. Starting from pure PC vesicles, k_{BP} decreased gradually with increased amount of PG until it leveled off to the value measured in the pure PG liposome (Figure 3), while $\Delta G°_{Q_A^-Q_B \rightarrow Q_AQ_B^-}$ changed from −77 to −89 meV (Table 2). Interestingly, the 50% change of k_{BP} was about 300 PG/RC, significantly larger than that of k_{AB}.

We carried out the same experiment with CL, a PG analogue of the diphosphatidylglycerol molecule, whose

Table 2: Reduced Cytochrome as Donor to RC Incorporated into LDAO Micelles and PC and PG Liposomes and Decomposition of Absorption Change Kinetics after Single-Flash Excitation (Figure 2)[a]

	A^0_{BP} (%)	k_{BP} (s^{-1})	A^0_{AP} (%)	k_{AP} (s^{-1})	$\Delta G°_{Q_A^-Q_B \rightarrow Q_AQ_B^-}$ (meV)
LDAO	93.1	0.83	6.9	10.0	−62
PC	98.0	0.38	2.0	8.3	−77
PC + cyt	40.3	0.49	1.1	8.3	
PG	71.0	0.13	29.0	4.0	−89
PG + cyt	41.6	0.12	21.0	3.7	

[a] A^0_{AP} and A^0_{BP} are the relative initial amplitudes of the fast and slow phase of the absorption change signals, respectively. k_{AP} and k_{BP} are the rate constants of the appropriate phases. $\Delta G°_{Q_A^-Q_B \rightarrow Q_AQ_B^-}$ was calculated as described in Materials and Methods. The maximum error is 10.5%.

attachment to the RC was identified in the crystal structure and its specific function in the RC photochemistry was already discussed (*11*, *31*, *32*). The effect of CL upon incorporation into the PC liposome is more complex than observed with PG (Figure 3). The change of rate constant of the back-reaction seems to follow two distinct titration phases: the first indicates a very tight association of CL with the RC, and the second refers to a much looser attachment between CL and the RC. Unfortunately, no single-component CL vesicles with the RC could be prepared; therefore, the exact evaluation of the data awaits further investigations.

$PQ_A^-Q_B^- \rightarrow PQ_AQ_B^{2-}$ Electron Transfer: k_{AB}(2). In the presence of the secondary donor, the RCs are able to perform more turnovers upon repetitive flash excitations. In living cells, cytochromes, either tightly bound to the RCs (e.g., in *Blc. viridis*) or solubilized in the extracytoplasmic compartment (e.g., in *Rb. sphaeroides*), donate electrons to the oxidized primary donor, P^+. Using reduced mitochondrial cytochrome c^{2+} (cyt c^{2+}) as the external electron donor to P^+ in our experiments, we have to keep in mind that cytochrome does not penetrate across the lipid layer (membrane); therefore, RCs with the periplasmic side faced to the aqueous (bulk) phase can undergo microsecond time scale P^+ rereduction by cyt c^{2+}. In the RCs of opposite orientation, P^+ can be rereduced by charge recombination with Q_A^- and/or Q_B^- only (Figure 2). From the fraction of the slow phase in the absorption kinetics at 603 nm we can deduce random orientation of the RCs (close to 50% inside out and right side out) in the liposome vesicles. The fractions of the slow-phase amplitudes were somewhat different in PG and PC liposomes. This can reveal either a tiny asymmetry of the orientation of the RC in the membrane (in PG vesicles this distribution favors the RCs with the dimer facing toward the interior of the liposomes) or a difference of the accessibility of cyt c^{2+} to P^+.

The rate constant k_{AB}(2) of the $PQ_A^-Q_B^- \rightarrow PQ_AQ_B^{2-}$ (second) electron transfer was determined from the kinetics of the absorption change measured at 450 nm after addition of cyt c^{2+} to the liposome suspension (data not shown). For the RCs in LDAO and liposomes made from the total lipid extract, the rate constants of the second electron transfer at 22.5 °C were 740 and 1300 s^{-1}, respectively (*18*). These values agree fairly well with the data of Taly et al. (*19*) measured at 13 and 30 °C. We observed, however, a larger rate constant in the PG liposome (1500 s^{-1}) and a significantly larger value in the PC environment (3300 s^{-1}) (Table 1).

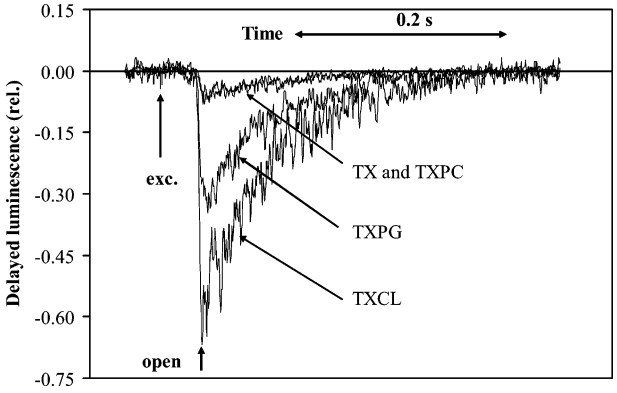

FIGURE 4: Delayed luminescence of the bacteriochlorophyll dimer of RC in Triton X-100 detergent micelles in the presence of PC, PG, and CL phospholipids. The delayed fluorescence of the samples was normalized to their prompt fluorescence. Conditions: 532 nm excitation; 920 nm detection; 3 μM RC, 10 mM Tris, 100 mM NaCl, and 0.02% TX-100, pH 8.0, and temperature 298 K.

Free Energy Change of the $P^*Q_A \rightarrow P^+Q_A^-$ Electron Transfer. The larger lifetime (and consequently the larger stabilization energy) of the $P^+Q_B^-$ charge pair in PG than in PC is really surprising. It is expected that the free energy levels (midpoints) of both the Q_B/Q_B^- and the Q_A/Q_A^- redox couples shift upon change of the phospholipid environment. The free energy of the Q_A/Q_A^- redox couple relative to the ground state, P/P^+, or the excited state, P^*/P^+, was determined from delayed fluorescence of the primary donor (bacteriochlorophyll dimer) after light excitation (*52*, *55*, *56*). We measured the kinetics of the delayed luminescence of RCs incorporated into TX detergent micelles without and with the addition of PC, PG, and CL lipids (Figure 4), together with DL emission from RC/lipid vesicles of single PC and PG components. After addition of PC to the TX/RC system, the $\Delta G°_{P^* \rightarrow Q_A^-}$ free energy change of the $P^+/P^* \rightarrow Q_A/Q_A^-$ reaction did not change significantly, in good agreement with recent results of Rinyu et al. (*55*), $\Delta(\Delta G°_{P^* \rightarrow Q_A^-})_{TX/PC} = (\Delta G°_{P^* \rightarrow Q_A^-})_{TX} - (\Delta G°_{P^* \rightarrow Q_A^-})_{TX+PC} =$ 2.3 meV, which was well within our experimental error of about ±3.3 meV. However, the free energy change was more pronounced if PG or CL was added to the TX/RC solution: $\Delta(\Delta G°_{P^* \rightarrow Q_A^-})_{TX/PG} = 40$ meV and $\Delta(\Delta G°_{P^* \rightarrow Q_A^-})_{TX/CL} = 55$ meV. If, however, the RC is incorporated in the vesicle made of a single phospholipid, the amplitude of the delayed luminescence increased relative to that of the TX/PC system: $\Delta(\Delta G°_{P^* \rightarrow Q_A^-})_{PC} = 29$ meV and $\Delta(\Delta G°_{P^* \rightarrow Q_A^-})_{PG} = 46$ meV.

The variation of the Q_A/Q_A^- free energy difference of the RC incorporated in the vesicle of mixed components was tracked by measurement of the delayed fluorescence. As we saw above, no major change was observed if PC was added to the TX/RC suspension, but the midpoint potential of the Q_A/Q_A^- redox couple significantly decreased in the single-component PC. An additional and large (20 meV) decrease was measured upon addition of PG to the PC/RC system, in contrast to CL, which did not modify the free energy level of the Q_A/Q_A^- redox couple measured in the PC vesicle. It is interesting to compare this finding with the change of the free energy gap of the interquinone electron transfer determined from the charge recombination kinetics. Here we

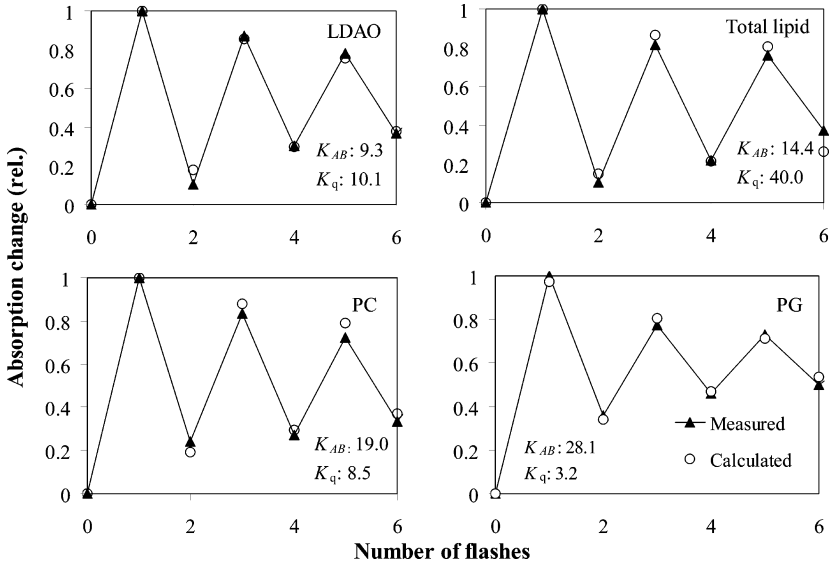

FIGURE 5: Oscillation of flash-induced absorption changes at 450 nm due to the formation and disappearance of semiquinones in RCs of *Rb. sphaeroides* incorporated into liposomes prepared from PC, PG, and total lipids extracted from chromatophores and in LDAO detergent micelles. The electron and quinone equilibrium constants, K_{AB} and K_q, respectively, were determined by best fit from the model described in refs *47* and *51*. Conditions: same as in Figure 1, except for 100 μM ferrocene. Flash repetition rate: 1 Hz (LDAO) and 0.2 Hz (total lipid, PC and PG). The data for the total lipid and LDAO samples were taken from Nagy et al. (*18*).

learned that the rate constant of the $P^+(Q_AQ_B)^- \rightarrow PQ_AQ_B$ charge recombination; consequently, the $\Delta G^\circ_{Q_A^-Q_B \rightarrow Q_{AB}^-}$ free energy decreased monotonically upon the addition of CL or PG to PC/RC vesicles (cf. Figure 3).

Multiple Turnover. After repetitive and saturating single-flash excitation in the presence of the exogenous donor to P^+, the absorption at 450 nm shows the periodic appearance and disappearance of the semiquinone Q^- (Figure 5). In detergent (LDAO) micelles, PC vesicles, and liposomes made from the total lipid extract of ICM, more than 20 (damped) oscillations can be measured. The degree of the damping is relatively small, and the absorption changes approach the steady state at about half of the maximum measured after the first flash (*57*−*59*). Much larger damping of the oscillation is observed in PG liposomes.

By using the simplest model appropriate to our conditions, the oscillation pattern is controlled by two parameters, K_{AB} and K_q, the one-electron equilibrium constants for Q_A/Q_B and quinone binding constant of the acceptor quinone complex, respectively (see Materials and Methods**)**. These parameters were calculated by the least-squares fitting procedure. K_{AB} increased significantly in the order LDAO micelles > total lipids > PC > PG. The quinone binding equilibrium constant, K_q, however, did not show this tendency. It was large in the liposomes made from the total lipid components of the ICM and very small in the PC, or even smaller in PG, resulting in a larger damping of the oscillation. Since the electron equilibrium constant, K_{AB}, is large in all samples, it appears that the oscillation pattern is determined by the equilibrium constant of the quinone binding/unbinding. The very small K_q in the PG vesicles can be the reason of the large damping of the oscillation in this sample. This finding is in good agreement with the relatively large fraction of P^+ that survived the first saturating flash excitation.

DISCUSSION

Artificial membranes provide a better approximation than the micellar system to determine the structural and functional parameters of the RCs. In many cases, the difference between the values obtained in the two systems is substantial. The lifetime of the $P^+Q_B^-$ charge pair is larger; the occupation of the Q_B site is higher, the K_{AB} is larger, the $\Delta G^0_{Q_A^-Q_B \rightarrow Q_{AB}^-}$ for the $P^+Q_A^-Q_B \rightarrow P^+Q_AQ_B^-$ electron transfer is more negative (*18*, *60*−*62*), and the free energy level of the Q_A/Q_A^- redox couple is higher in the natural membrane than in detergent micelles (*63*, *64*). Although some kinetic and thermodynamic parameters obtained in artificial liposomes do not coincide with those in the native membrane, the study of RC embedded in vesicles can lead us closer to understanding the in vivo situation. This work is one step in this direction.

Protein Dynamics and Charge Compensating Effects in Lipid Membranes. There are increasing amounts of evidence that after light excitation the formation of the donor−acceptor charge pair, $P^+Q_A^-$, and the forward electron transfer from Q_A^- to Q_B induce charge compensating relaxation rearrangements accompanying conformation movements within the protein. Different conformation states were identified after crystallization of the RCs under dark and light conditions (*14*, *65*). The structure of the *Rb. sphaeroides* L209PY mutant, in which proline at the L209 position was mutated to tyrosine, showed that Q_B could be trapped in the proximal position even in the charge-neutral state (*42*, *65*). Photoacoustic experiments provided direct proof for conformation changes of the RCs after the primary charge pair formation (*66*, *67*) and also after the $Q_A^-Q_B \rightarrow Q_AQ_B^-$ electron transfer (*68*). The appearance of long-lived components in $P^+Q^- \rightarrow PQ$ recombinational kinetics due to freezing under illumination (*50*) to continuous illumination (*69*) or to mutation (*70*) was interpreted by different conformation states of the RCs. The protein relaxation after flash excitation can cover a large time range (up to 100 ms), as revealed recently by delayed fluorescence measurements (*71*). The coupling of the electron transport and protein dynamics has been the subject of several interesting works (*61*, *72*).

The optical difference spectra of $P^+Q_A^-/PQ_A$ and/or $P^+Q_B^-/PQ_B$ reflect the electrochromic response of the BPheo absorption due to the different local electrostatic field around $BPheo_L$ and $BPheo_M$ (*53*, *73*, *74*). The electron transfer induces rearrangements of partial charges and/or hydrogen-bonding networks within the protein (*75*) and might be kinetically gated by these conformational rearrangements (*3*, *15*, *39*, *53*). Probably the second electron transfer is also affected by structural reorganization of the protein (*18*, *19*, *68*).

The transient absorption signal of RCs in PC and PG liposomes at 771 nm fits the biphasic model of the first electron transfer (*3*, *15*, *39*, *53*). This finding is consistent with earlier results that transient absorption change at 398 nm associated with the $P^+Q_A^-Q_B \rightarrow P^+Q_AQ_B^-$ electron transfer did not show components of 2−40 μs lifetimes if Q_A and Q_B were reconstituted with UQ_{10} (*76*). The observed lifetimes of the fast phase of a few tens of microseconds do not differ significantly in LDAO, PC, and PG in our experiments (Figure 1 and Table 1). This is not the case with the slow component that includes the effect of charge relaxation. Our results indicate that the charge compensation effects are somewhat larger and significantly faster in the PC than in the PG environment. These processes include possible rearrangements of the hydrogen-bonding network, i.e., protonation state (pattern) of amino acid side chains including Glu L212 and water molecules, and a change in the van der Waals contacts within the protein via accompanying conformational movements.

Recently, Remy et al. suggested a possible mechanism of the $Q_A^-Q_B \rightarrow Q_AQ_B^-$ electron transfer between the primary and secondary quinones (*77*). These authors concluded that the fast proton uptake by appropriate amino acids in about 12 and 150 μs and not the conformational movement induces the fast reduction of Q_B by an alternative transient redox couple, X, followed by slower electron transfer from Q_A^- to this intermediate species. Although the crystal structure from Stowell et al. (*14*) may include a dramatic movement of the secondary quinone from the distal to the proximal position prior to the Q_B reduction, there is no direct evidence for coupling between the $Q_A^-Q_B \rightarrow Q_AQ_B^-$ electron transfer and this flip-flop movement of Q_B. Indeed, Remy and coworkers and very recently Breton (*40*) and Baxter et al. (*41*) provided experimental evidence that the electron transfer from Q_A^- to Q_B is unrelated to the location of Q_B. Either the single step or the X-mediated mechanism is valid, the change of the electrostatics on the surface of the protein in the close vicinity of the quinones and in the surrounding hydrogen-bonding network, may alter the pK_a's of key amino acids and the redox midpoint potential of Q_A/Q_A^- and/or Q_B/Q_B^- essentially. Consequently, the kinetics and the energetics of the first and second electron transfer may also change.

Energetics of the Quinone Acceptor Complex. On the basis of DL measurements on the millisecond time range, we experienced a significant shift of the free energy of the Q_A/Q_A^- redox couple by 55 meV upon addition of CL to the TX solution to the direction found in the native membrane. No such effect was seen if PC was added to the TX micellar solution. These results are in good agreement with those obtained by Rinyu et al. (*55*). A moderate decrease of 40.3 meV was seen in the TX/PG/RC solution. Despite these observations in mixed detergent/phospholipid systems, these anionic lipids showed different effects if the RCs were embedded into PC vesicles. More specifically, no further change was observed by CL in the CL/PC/RC system, but surprisingly, addition of PG increased the free energy of Q_A by about 20 meV in the PG/PC/RC system. Note that PC and PG alone increase the midpoint potential of the Q_A/Q_A^- redox couple by 29 and 46 meV, respectively, in the corresponding single-component vesicle.

Table 3: Distances between Some Characteristic Atoms of the Secondary Quinone, UQ_{10} 2, Phosphatidylcholine, PC 2, and the Bacteriopheophytin, BPheo 1, in the Inactive Branch of the Cofactors[a]

UQ_{10} 2			BPheo 1		
O5	O2	PC 2	O1D 43	O2D 44	NA5
8.1	6.1	O2 35	8.9	8.0	10.3
7.8	7.7	O3 36	8.1	6.2	8.0
7.7	8.8	O11 37	7.7	6.0	6.2
10.1	6.9	O31 38	10.1	9.7	12.1
12.2	11.0	O1P 39	5.65	6.0	6.3
12.4	10.8	O2P 40	7.5	7.6	8.2
10.3	8.7	O3P 41	5.4	5.3	7.0
12.6	10.3	O4P 42	5.38	8.45	8.65
14.5	11.0	N30 34	9.6	10.3	12.3

[a] O2 and O5 are the proximal and distal oxygen atoms of Q_B. O1D, O2D, and NA5 are oxygen and nitrogen atoms attached to the tetrapyrrole rings of the BPheo. O2 35 and O3 36 are the ether and O11 37 and O31 38 are the carbonyl oxygen atoms of the ester bond between the acyl chains and the glycerol. O1 4P oxygen atoms are bound to phosphorus. N30 34 is the quaternary N atom of the PC 2. The distances were calculated according to the RC structure downloaded from the Protein Data Bank. The PDB ID code of the file is 1M3X.

To rationalize these observations coming from specific RC/phospholipid interactions, we turn to crystal structures that became recently available. The RC structure reported by Camara-Artigas et al. (*32*) shows that CL binds somewhat closer to the Q_A than to the Q_B site, although the difference is not too large (1M3X entry code in the Protein Data Bank; www.rcsb.org). The shortest distances (oxygen to oxygen) from CL to Q_A and Q_B are about 17 and 20 Å, respectively. It is noteworthy to remark that the edge to edge distance between CL and PC in this structure (about 25 Å) does not differ very much from those of CL to Q_A and CL to Q_B. The bonding interactions between RC and CL are described in detail, for example, by McAuley et al. (*11*) and Camara-Artigas et al. (*32*). Similar consideration can be made in the RC/PC system, although the PC binds closer to the secondary quinone site than to the primary quinone site of the RC. The distances and part of the hydrogen-bonding network are summarized in Table 3 and demonstrated in Figure 6. Both CL and PC bind to specific surface groups of the protein, and there is no indication that their binding sites remain saturated after crystallization. The observed heterogeneity regarding lipid-containing and lipid-free RCs after purification supports this view (*24*). In addition to the strong binding interactions between these lipids and RCs, several weaker binding sites may be in function, which can lose their bound lipids during the purification procedure. PC is a zwitterionic lipid, and the positive and negative charges, unlike in LDAO, are far from each other. Therefore, they can interact differently with the RC. Introduction of positive or negative charges or both charges can modify the binding interaction of the anionic lipid if PC is present.

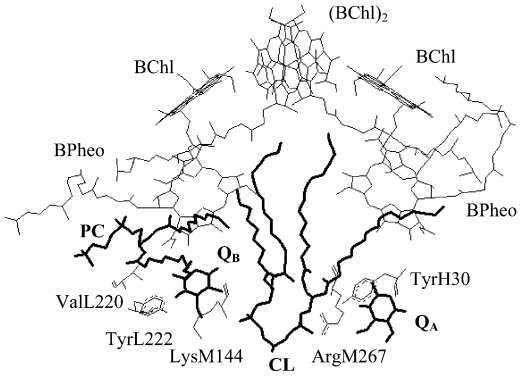

FIGURE 6: Structure of the binding area of PC and CL with the primary and secondary quinones (thick lines) and nearby amino acid residues. The redox-active cofactors, Bchl dimer and monomers, and the two Bpheo molecules are also indicated (thin lines). For better viewing, the polyisoprene tail of the Q_A and Q_B was truncated. The plot was drawn from the RC structure downloaded from the Protein Data Bank (www.rcsb.org). The PDB ID code of the file is 1M3X.

Figure 7 shows the network of the bonding interactions of amino acids and water molecules in the RC around the PC and Q_B binding site. Parts of amino acids of the L and M subunits in the Q_B loop and the types of interactions are indicated. The tertiary structure of the photosynthetic RCs is stabilized primarily by efficient atomic packing and helix−dipole interactions (*78*). The polar interactions, salt bridges, and hydrogen-bonding interactions between the subunits do not play a significant role in the intramembrane structure; the coupling between the interhelical connections outside the membrane -spanning regions, however, can be more important. PC binds close to one of these regions that interconnects the L-D and L-de helices (L-D is a transmembrane helix, and L-de is parallel to the membrane surface). This extended hydrogen-bonding network involving the amino acid side chains as well as peptide-bonding nitrogen and oxygen atoms, also in the M subunits close to the amino terminus of this subunit, is very sensitive to the electrostatics of the protein surface. Note that the shortest distance between the PC and the nearby amino acid, Val L220, is 4.12 Å only. Camara-Artigas et al. (*32*) discussed the possible effect of PC on the electrostatics of BPheo in the inactive branch of the RC. In addition to this possible interaction, the effect of PC on Q_B through the rearrangement of the hydrogen-bonding network cannot be excluded. Q_A and Q_B, together with the iron cluster, work as a structural and functional unit, called the "acceptor quinone complex" (*55*, *75*). Because of the extended hydrogen-bonding network, it is expected that changes in the Q_B electrostatics modify the function of the Q_A side as well. Similar consideration can be drawn for the other phospholipids (CL and PG) used in our experiments.

The rate constants of the observed electron transfer steps are all sensitive to the environmental factors (*18*, *19*). The rate constant of the $P^+Q_B^- \rightarrow PQ_B$ charge recombination depends on the local electrostatics of the Q_B pocket that can be modified by the lipid environment. The slow component of the first interquinone electron transfer kinetics is attributed to protein relaxation (ionic and protonic rearrangement) and should be sensitive to the lipids attached (or bound) to the protein. The rate constant of the second electron transfer depends both on the fraction of the protonated semiquinone (Q_BH) and on the intrinsic rate constant of the second interquinone electron transfer, k_e: $k_{AB}(2) = f(Q_BH)k_e$ (*79*). Both factors (the p*K* of the semiquinone and the free energy gap controlling k_e) can be exposed to changes due to the modified environment.

Quinone Binding. The contribution of the electron equilibrium constant, K_{AB}, between the $Q_A^-Q_B$ and $Q_AQ_B^-$ states and the quinone equilibrium constant, K_q, between the RC fractions of bound and unbound Q_B is tested by the binary

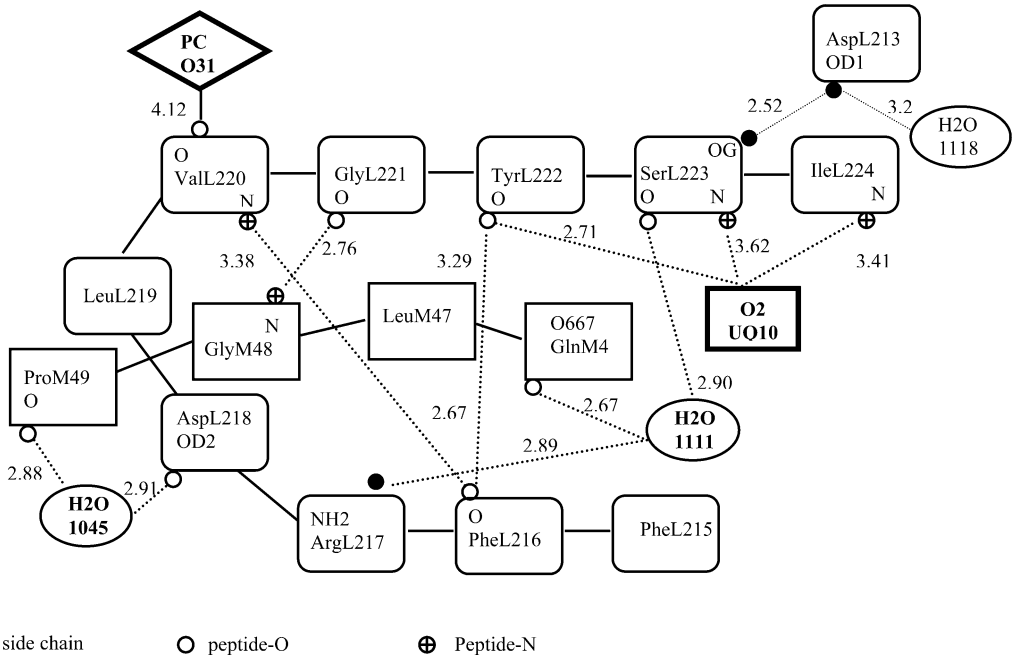

FIGURE 7: Bonding interactions of amino acids and water molecules in the RC around the PC and Q_B binding site. Parts of amino acids of the L and M subunits in the Q_B loop and the types of interactions are indicated: covalent peptide bonds (solid line) and possible hydrogen-bonding interactions (the distance is smaller than 3.5 Å, dotted lines). Open and filled circles represent the appropriate peptide and side chain atoms, respectively. The distances were calculated according to the RC structure downloaded from the Protein Data Bank (www.rcsb.org). The PDB ID code of the file is 1M3X.

oscillation of the semiquinone absorption after repetitive flash excitation. Since the lifetime of the $P^+Q_B^-$ state and the occupation of the Q_B site is high, it is expected that the damping of the oscillation pattern in PC and PG is comparable to that in the total lipid liposomes and in LDAO micelles (*18*). However, both the damping and the steady-state level are high in PG. On the basis of model calculations (Figure 5), we obtained a small ($K_q = 3.2$) quinone binding constant for RC embedded in PG liposome which includes that 34.2% of the RCs do not bind Q_B during the sequence of illumination. This value agrees fairly well with the fraction of the fast-phase amplitude of the charge recombination in the PG environment (Figure 2). We can argue for two possible reasons of this behavior. (1) Embedded into the PG liposome, the RC may have preferred orientations that make the accessibility to the bulk phase (and thus to the external donor) asymmetric. (2) Due to structural and/or kinetic reasons, the quinones from the pool become less available to the Q_B site; i.e., their accessibility is restricted in the PG liposome.

PG added to PC bilayer vesicles that mimic the in vivo conditions decreased both the rate constants of $Q_A^-Q_B \rightarrow Q_AQ_B^-$ electron transfer and $P^+(Q_AQ_B)^- \rightarrow P(Q_AQ_B)$ charge recombination. The rate constants as a function of relative PG concentration (Figure 3) followed a Michaelis−Menten-type mechanism, indicating establishment of equilibrium between bound and free PG in both cases. CL has somewhat different behavior. The titration curve suggests two types of binding sites to the RCs. The high-affinity site is close to the stoichiometric ratio, and the other site becomes effective at a higher concentration range. The strong binding site can be easily saturated and remains saturated even after different preparation processes. The low-affinity binding site has a few hundredths of CL/RC for half-saturation. It is important to note that care must be taken when liposomes are prepared from CL. First, the concentration of CL in the bacterial membrane is smaller than that of PC and PG. A higher concentration of CL can help us to understand the effect of anionic phospholipids in charge stabilization but has not much physiological significance. Second, the CL/RC intact vesicular system cannot be made from pure CL.

Anionic lipids (CL and PG) can form contact surfaces between monomers of membrane proteins and contribute to production of multimers. Although the dimer formation of RCs of *Rb. sphaeroides* in vivo membranes is still questionable, recent crystallographic data suggest that CL facilitates molecular contacts in dimers of RCs (*80*) and stabilization of cytochrome *c* oxidase (*81*). PG is also involved in the oligomerization of PS I reaction centers (*82*) and the stabilization of PS II dimers (*83*), and within the map of the recently determined X-ray structure of PS II (*84*) there is density that can accommodate two PG molecules at the interface between the two monomers (James Barber and So Iwata, personal communication). Change of the electrostatic effects due to alteration of surface contacts is indicative of modified electron transfer parameters, which were also proved by the effect of phase transition of DMPC/RC vesicles (*19*).

CONCLUSION

This study provides direct evidence for the specific functional role of PG, a characteristic lipid of the photosynthetic membrane both in eucaryotic and prokaryotic organisms, probably by binding to specific site(s) in the RC protein. Data presented also for CL support the idea that one of the effects of PG includes the stabilization of light-induced charge(s) in photosynthetic energy conversion. PG increases significantly the lifetime of the $P^+Q_B^-$ state and the free energy gap that drives the Q_A^- to Q_B electron transfer. The rate constant of the Q_A^- to Q_B electron transfer depends not only on the redox state of Q_B but also on the microenvironment of the Q_B site. It is shown that PG affects both the stabilization energy of Q_B^- (the free energy of the $P^+Q_A^-Q_B$ state will be higher while that of the $P^+Q_AQ_B^-$ state will be lower) and the quinone binding/unbinding equilibrium. The free energy levels of $Q_A^-Q_B$ and $Q_AQ_B^-$ redox states of the RC under different lipid conditions can be constructed (Figure 8). The differential effect of anionic lipids on the Q_A/Q_A^- energetics in the lipid membrane indicates that different components of the ICM interact to regulate the protein function.

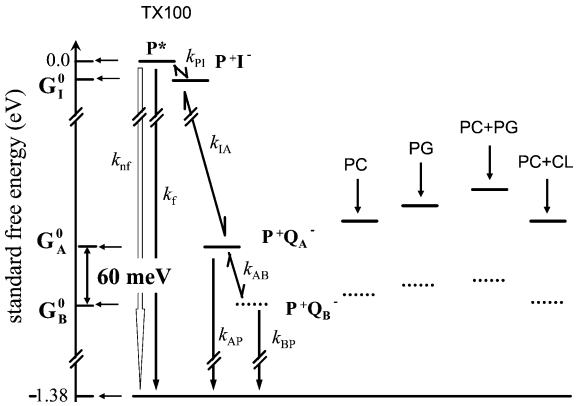

FIGURE 8: Schematic representation of the free energy levels of the $P^+Q_A^-$ (solid line) and $P^+Q_B^-$ (dotted line) redox couples compared to that of the P* in the photosynthetic RC in different environments determined from delayed fluorescence of the dimer and from charge recombination kinetics (see Materials and Methods). k_f, k_{nf}, k_{PI}, and k_{IA} are the rate constants of fluorescence emission, radiationless transition, P^+I^- charge separation, and $P^+I^- \rightarrow P^+Q_A^-$ electron transfer, respectively. P^+I^- is the primary charge-separated radical pair (I = BPheo). Other symbols are defined in the text.

ACKNOWLEDGMENT

Dr. Zoltán Gombos (BRC, Szeged, Hungary) is thanked for careful reading of the manuscript and for helpful comments. We are very much indebted to the reviewers for the helpful comments. Thanks are due to Judit Tóth for technical support.

REFERENCES

1. Sebban, P., Maróti, P., and Hanson, D. K. (1995) Electron and proton transfer to the quinones in bacterial photosynthetic reaction centers: Insight from combined approaches of molecular genetics and biophysics, *Biochimie 77*, 677−694.
2. Allen, J. P., and Williams, J. C. (1998) Photosynthetic reaction centers, *FEBS Lett. 438*, 5−9.
3. Okamura, M. Y., Paddock, M. L., Graige, M. S., and Feher, G. (2000) Proton and electron transfer in bacterial reaction centers, *Biochim. Biophys. Acta 1458*, 148−163.
4. Paddock, M. L., Feher, G., and Okamura, M Y. (2003) Proton transfer pathways and mechanism in bacterial reaction centers, *FEBS Lett. 555*, 45−50.

5. Wraight, C. A. (2004) Proton and electron transfer in the acceptor quinone complex of photosynthetic reaction centers from *Rhodobacter sphaeroides*, *Frontiers Biosci. 9*, 309−337.
6. Wraight, C. A., and Clayton, R. (1974) The absolute quantum efficiency of bacteriochlorophyll photooxidation in reaction centers of *Rhodopseudomonas sphaeroides*, *Biochim. Biophys. Acta 333*, 246−260.
7. Rautter, J., Lendzian, F., Schulz, C., Fetsch, A., Kuhn, M., Lin, X., Williams, J. C., Allen, J. P., and Lubitz, W. (1995) ENDOR studies of the primary donor cation radical in mutant reaction centers of *Rhodobacter sphaeroides* with altered hydrogen-bond interactions, *Biochemistry 34*, 8130−8143.
8. Muh, F., Rautter, J., and Lubitz, W. (1997) Two distinct conformations of the primary electron donor in reaction centers from *Rhodobacter sphaeroides* revealed by ENDOR/TRIPLE-spectroscopy, *Biochemistry 36*, 4155−4162.
9. McPherson, P. H., Okamura, M., Y., and Feher, G. (1990) Electron transfer from the reaction center of *Rhodobacter sphaeroides* to the quinone pool: doubly reduced Q_B leaves the reaction center, *Biochim. Biophys. Acta 1016*, 289−292.
10. Fathir, I., Mori, T., Nogi, T., Kobayashi, M., Miki, K., and Nozawa, T. (2001) Structure of the H subunit of the photosynthetic reaction center from the thermophilic purple bacterium, *Thermochromatium tepidum*—Implications for the specific binding of the lipid molecule to the membrane protein complex, *Eur. J. Biochem. 268*, 2652−2657.
11. McAuley, K. E., Fyfe, P. K., Ridge, J. P., Isaacs, N. W., Cogdell, R. J., and Jones, M. R. (1999) Structural details of interaction between cardiolipin and an integral membrane protein, *Proc. Natl. Acad. Sci. U.S.A. 96*, 14706−14711.
12. Ermler, U., Fritzsch, G., Buchanan, S. K., and Michel, H. (1994) Structure of the photosynthetic reaction-center from *Rhodobacter-sphaeroides* at 2.65 Å resolution—cofactors and protein−cofactor interactions, *Structure 2*, 925−936.
13. Ermler, U., Michel, H., and Schiffer, M. (1994) Structure and function of the photosynthetic reaction-center from *Rhodobacter-sphaeroides*, *J. Bioenerg. Biomembr. 26*, 5−15.
14. Stowell, M. H. B., McPhillips, T. M., Rees, D. C., Soltis, S. M., Abresh, E., and Feher, G. (1997) Light induced structural changes in photosynthetic reaction center: implications for mechanism of electron−proton transfer, *Science 276*, 812−816.
15. Tiede, D. M., Vázquez, J., Córdova, J., and Marone, P. (1996) Time-resolved electrochromism associated with the formation of quinone anions in the *Rhodobacter sphaeroides* R26 reaction center, *Biochemistry 35*, 10763−10775.
16. Lavergne, J., Matthews, C., and Ginet, N. (1999) Electron transfer on the acceptor side of the reaction center in chromatophores of *Rhodobacter capsulatus*. Evidence for direct protonation of the semiquinone state of Q_B, *Biochemistry 38*, 4542−4552.
17. Sebban, P., and Wraight, C. A. (1989) Heterogeneity of the $P^+Q_A^-$ recombination kinetics in reaction centers from *Rhodopseudomonas viridis*: the effects of pH and temperature, *Biochim. Biophys. Acta 974*, 54−65.
18. Nagy, L., Fodor, E., Tandori, J., Rinyu, L., and Farkas, T. (1999) Lipids affect the charge stabilization in wild type and mutant reaction centers of *Rhodobacter sphaeroides*, *Aust. J. Plant Physiol. 25*, 465−473.
19. Taly, A., Baciou, L., and Sebban, P. (2002) The DMPC lipid phase transition influences differently the first and the second electron transfer reactions in bacterial reaction centers, *FEBS Lett. 532*, 91−96.
20. Donohue, T. J., Cain, B. D., and Kaplan, S. (1982) Alteration in the phospholipid composition of *Rhodopseudomonas sphaeroides* and other bacteria induced by Tris, *J. Bacteriol. 152*, 595−606.
21. Wood, B. J. B., Nichols, B. W., and James, A. T. (1965) The lipids and fatty acid metabolism of photosynthetic bacteria, *Biochim. Biophys. Acta 106*, 261−273.
22. Steiner, S., Sojka, G. A., Conti, S. F., Gest, H., and Lester, R. L. (1970) Modification of membrane composition in growing photosynthetic bacteria, *Biochim. Biophys. Acta 203*, 571−574.
23. Onishi, J. C., and Niederman, R. (1982) *Rhodopseudomonas sphaeroides* membranes: Alterations in phospholipid composition in aerobically and phototrophically grown cells, *J. Bacteriol. 149*, 831−839.
24. Fyfe, P. K., Isaacs, N. W., Cogdell, R., and Jones, M. (2004) Disruption of a specific molecular interaction with a bound lipid affects the thermal stability of the purple bacterial reaction centre, *Biochim. Biophys. Acta 1608*, 11−22.
25. Sebban, P., Parot, P., Baciou, L., Mathis, P., and Verméglio, A. (1991) Effects of low temperature and lipid rigidity on the charge recombination process in *Rps. viridis* and *Rb. sphaeroides* reaction centers, *Biochim. Biophys. Acta 1057*, 109−114.
26. Overfield, R. E., and Wraight, C. A. (1980) Oxidation of cytochromes c and c_2 by bacterial photosynthetic reaction centers in phospholipid vesicles: 1. Studies with natural membranes, *Biochemistry 19*, 3322−3327.
27. Overfield, R. E., and Wraight, C. A. (1980) Oxidation of cytochromes c and c_2 by bacterial photosynthetic reaction centers in phospholipid vesicles: 2. Studies with negative membranes, *Biochemistry 19*, 3328−3334.
28. Linscheid, M. L., Diehl, B. W., Övermöhle, M., Riedl, I., and Heinz, E. (1997) Membrane lipids of *Rhodopseudomonas viridis*, *Biochim. Biophys. Acta 1347*, 151−163.
29. Lancaster, C. R. D., and Michel, H. (1997) The coupling of light-induced electron transfer and proton uptake as derived from crystal structures from reaction centers of *Rhodopseudomonas viridis* modified at the binding site of the secondary quinone, Q_B, *Structure 5*, 1339−1359.
30. Agostiano, A., Milano, F., and Trotta, M. (1999) Investigation on the detergent role in the function of secondary quinone in bacterial reaction centers, *Eur. J. Biochem. 262*, 358−364.
31. Wakeham, M. C., Sessions, R. B., Jones, M. R., and Fyfe, P. K. (2001) Is there conserved interaction between cardiolipin and the type II bacterial reaction center, *Biophys. J. 80*, 1395−1405.
32. Camara-Artigas, A., Brune, D., and Allen, J. (2002) Interactions between lipids and bacterial reaction centers determined by protein crystallography, *Proc. Natl. Acad. Sci. U.S.A. 99*, 11055−11060.
33. Nogi, T., Fathir, I., Kobayashi, M., Nozawa, T., and Miki, K. (2000) Crystal structures of photosynthetic reaction centers and high potential iron−sulfur protein from *Thermochromatium tepidum*; thermostability and electron transfer, *Proc. Natl. Acad. Sci. U.S.A. 97*, 13561−13566.
34. Kruse, O., and Schmid, G. H. (1995) The role of phosphatidylglycerol as a functional effector and membrane anchor of the D1-core peptide from photosystem II-particles of the cyanobacterium *Oscillatoria chalybea*, *Z. Naturforsch. 50c*, 380−390.
35. Hagio, M., Gombos, Z., Várkonyi, Zs., Masamoto, K., Sato, N., Tsuzuki, M., and Wada, H. (2000) Direct evidence for requirement of phosphatidylglycerol in photosystem II of photosynthesis, *Plant Physiol. 124*, 795−804.
36. Sato, N., Hagio, M., Wada, H., and Tsuzuki, M. (2000) Requirement of phosphatidylglycerol for photosynthetic function in thylakoid membranes, *Proc. Natl. Acad. Sci. U.S.A. 97*, 10655−10660.
37. Gombos, Z., Várkonyi, Zs., Hagio, M., Iwaki, M., Kovács, L., Masamoto, K., Itoh, S., and Wada, H. (2002) Phosphatidylglycerol requirement for the function of electron acceptor plastoquinone Q_B in the photosystem II reaction center, *Biochemistry 41*, 3796−3802.
38. Aro, E. M., Virgin, L., and Andersson, B. (1993) Photoinhibition of photosystem-2—inactivation, protein damage and turnover, *Biochim. Biophys. Acta 1143*, 113−134.
39. Graige, M. S., Feher, G., and Okamura, M. Y. (1998) Conformational gating of the electron transfer reaction $Q_A^{-\bullet}Q_B \rightarrow Q_AQ_B^{-\bullet}$ in bacterial reaction centers of *Rhodobacter sphaeroides* determined by driving force assay, *Proc. Natl. Acad. Sci. U.S.A. 95*, 11679−11684.
40. Breton, J. (2004) Absence of large-scale displacement of quinone Q_B in bacterial photosynthetic reaction centers, *Biochemistry 43*, 3318−3326.
41. Baxter, R. H. G., Ponomarenko, N., Šrajer, V., Pahl, R., Moffat, K., and Norris, J. R. (2004) Time-resolved crystallographic studies of light-induced structural changes in the photosynthetic reaction center, *Proc. Natl. Acad. Sci. U.S.A. 101*, 5982−5987.
42. Kuglstatter, A., Ermler, U., Michel, H., Baciou, L., and Fritsch, G. (2001) X-ray structure analyses of photosynthetic reaction center variants from *Rhodobacter sphaeroides*: structural changes induced by point mutations at position L209 modulate electron and proton transfer, *Biochemistry 40*, 4253−4260.
43. Ormerod, J. G., Ormerod, K. S., and Gest, H. (1961) Light-dependent utilization of organic compounds and photoproduction of molecular hydrogen by photosynthetic bacteria; relationships with nitrogen metabolism, *Arch. Biochem. Biophys. 94*, 449−463.
44. Tandori, J., Nagy, L., Puskás, A., Droppa, M., Horváth, G., and Maróti, P. (1995) The $Ile^{L229} \rightarrow$ Met mutation impairs the quinone binding to the Q_B-pocket in reaction centers of *Rhodobacter sphaeroides*, *Photosynth. Res. 45*, 135−146.

45. Ollivon, M., Lesieur, S., Grabielle-Madelmont, C., and Paternostre, M. (2000) Vesicle reconstitution from lipid-detergent mixed micelles, *Biochim. Biophys. Acta 1508*, 34−50.
46. Trotta, M., Milano, F., Nagy, L., and Agostiano, A. (2002) Response of membrane protein to the environment: the case of photosynthetic reaction centre, *Mater. Sci. Eng., C 22*, 263−267.
47. Tandori, J., Nagy, L., and Maróti, P. (1991) Semiquinone oscillation as a probe of quinone/herbicide binding in bacterial reaction centers, *Photosynthetica 25*, 159−166.
48. Lakatos, M., Groma, G. I., Ganea, C., Lanyi, J. K., and Váró, G. (2002) Characterization of the azide-dependent bacteriorhodopsin-like photocycle of salinarum halorhodopsin *Biophys. J. 82*, 1687−1695.
49. Wraight, C. A., and Stein, R. R. (1983) Redox equilibrium in the acceptor quinone complex of isolated reaction centers and the mode of action of orthophenantroline, *FEBS Lett. 113*, 73−77.
50. Kleinfeld, D., Okamura, M. Y., and Feher, G. (1984) Electron transfer in reaction centers of *Rhosopseudomonas sphaeroides*. I. Determination of the charge recombination pathway of $D^+Q_AQ_B^-$ and free energy and kinetic relations between $Q_A^-Q_B$ and $Q_AQ_B^-$, *Biochim. Biophys. Acta 766*, 126−140.
51. Halmschlager, A., Tandori, J., Trotta, M., Rinyu, L., Pfeiffer, I., and Nagy, L. (2002) A mathematical model for the quinone-herbicide competition in the reaction centers of *Rhodobacter sphaeroides*, *Funct. Plant Biol. 29*, 1−7.
52. Turzo, K., Laczkó, G., Filus, Z., and Maróti, P. (2000) Quinone-dependent delayed fluorescence from the reaction center of photosynthetic bacteria, *Biophys. J. 79*, 14−25.
53. Tiede, D. M., Utschig, L., Hanson, D. K., and Gallo, D. M. (1998) Resolution of electron and proton transfer events in the electrochromism associated with quinone reduction in bacterial reaction centers, *Photosynth. Res. 55*, 267−273.
54. Okamura, M. Y., Isaacson, R. A., and Feher, G. (1975) Primary acceptor in bacterial photosynthesis: Obligatory role of ubiquinone in photoactive reaction centers of *Rhodopseudomonas sphaeroides*, *Proc. Natl. Acad. Sci. U.S.A. 72*, 3491−3495.
55. Rinyu, L., Martin, E., Takahashi, E., Maróti, P., and Wraight, C. (2004) Modulation of the free energy of the primary quinone acceptor (QA) in reaction centers from *Rhodobacter sphaeroides*: contributions from the protein and protein−lipid (cardiolipin) Interaction, *Biochim. Biophys. Acta 1655*, 93−101.
56. Arata, H., and Parson, W. (1981) Delayed fluorescence from *Rhodopseudomonas sphaeroides* reaction centers; Enthalpy and free energy changes accompanying electron transfer from P-870 to quinones, *Biochim. Biophys. Acta 638*, 201−209.
57. Kleinfeld, D., Abresch, E. C., Okamura, M. Y., and Feher, G. (1984) Damping oscillations in the semiquinone absorption in reaction centers after successive flashes, *Biochim. Biophys. Acta 756*, 406−409.
58. Verkhovskii, M. I., Kaurov, B. S., Rubin, A. B., and Shinkarev, V. P. (1981) Kinetics of conversion of ubisemiquinone in primary reactions of bacterial photosynthesis, *Mol. Biol. (Moscow) 15*, 589−600.
59. Shinkarev, V. P., Verkhovskii, M. I., Kaurov, B. S., and Rubin, A. B. (1981) The kinetic model of two electron gate in photosynthetic reaction center of bacteria, *Mol. Biol. (Moscow) 15*, 743−844.
60. Maróti, P. (1991) Electron transfer and proton uptake of photosynthetic bacterial reaction centers reconstituted in phospholipid vesicles, *J. Photochem. Photobiol., B 8*, 263−277.
61. Palazzo, G., Mallardi, A., Giustini, M., Berti, D., and Venturolli, G. (2000) Cumulant analysis of charge recombination kinetics in bacterial reaction centers reconstituted into lipid vesicles, *Biophys. J. 79*, 1171−1179.
62. Milano, F., Agostiano, A., Mavelli, F., and Trotta, M. (2003) Kinetics of quinone binding reaction at the Q_B site of reaction centers from the purple bacteria *Rhodobacter sphaeroides* reconstituted in liposomes, *Eur. J. Biochem. 270*, 4595−4605.
63. Wraight, C. A. (1981) Oxidation−reduction physical chemistry of the acceptor quinone complex in bacterial reaction centres: evidence for a new model of herbicide activity, *Isr. J. Chem. 21*, 348−354.
64. Dutton, P. L., Leigh, J. S., and Wraight, C A. (1973) Direct measurement of the midpoint potential of the primary electron acceptor in *Rhodopseudomonas sphaeroides in situ* and in the isolated state: some relationships with pH and o-phenantroline, *FEBS Lett. 36*, 169−173.
65. Fritzsch, G., Koepke, J., Diem, R., Kuglstatter, A., and Baciou, L. (2002) Charge separation induces conformational changes in the photosynthetic reaction center of purple bacteria, *Acta Crystallogr., Sect. D: Biol. Crystallogr. 58*, 1661−1663.
66. Mauzerall, D. C., Gunner, M. R., and Zhang, J. W. (1995) Volume contraction on photoexcitation of the reaction center from *Rhodobacter sphaeroides* R-26: Internal probe of dielectrics, *Biophys. J. 68*, 275−280.
67. Brumfeld, V., Nagy, L., Kiss, V., and Malkin, S. (1999) Wide-frequency hydrophone detection of laser-induced photoacoustic signals in photosynthesis, *Photochem. Photobiol. 70*, 607−615.
68. Nagy, L., Kiss, V., Brumfeld, V., and Malkin, S. (2001) Thermal and structural changes of photosynthetic reaction centers characterized by photoacoustic detection with a broad frequency band hydrophone, *Photochem. Photobiol. 74*, 81−87.
69. Kálmán, L., and Maróti, P. (1997) Conformation-activated protonation in reaction centers of the photosynthetic bacterium *Rhodobacter sphaeroides*, *Biochemistry 36*, 15269−15276.
70. Andrasson, U., Carlsson, T., and Andreasson, L. E. (2003) Spectroscopic characterization of a semi-stable, charge-separated state in Cu^{2+}-substituted reaction centers from *Rhodobacter sphaeroides*, *Biochim. Biophys. Acta 1607*, 45−52.
71. Filus, Z., Laczkó, G., Wraight, C. A., and Maróti, P. (2004) Delayed fluorescence from photosynthetic reaction center measured by electronic gating of the photomultiplier, *Biopolymers 74*, 92−95.
72. McMahon, B. H., Müller, J. D., Wraight, C. A., and Nienhaus, G. U. (1998) Electron transfer and protein dynamics in the photosynthetic reaction center, *Biophys. J. 74*, 2567−2587.
73. Franken, R. M., Shkuropatov, A. Y., Franke, C., Neerken, S., Gast, P., Shuvalov, V. A., Hoff, A. J., and Aartsma, T. J. (1997) Reaction centers of *Rhodobacter sphaeroides* R-26 with selective replacement of becteriopheophytin by pheophytin *a* Part I: Characterisation of steady state absorbance and circular dichroism, and of the $P^+Q_A^-$ state, *Biochim. Biophys. Acta 1319*, 242−250.
74. Shopes, R. J., and Wraight, C. A. (1985) The acceptor quinone complex of *Rhodopseudomonas viridi*s reaction centers, *Biochim. Biophys. Acta 806*, 348−356.
75. Sebban, P., Maróti, P., Schiffer, M., and Hanson, D. (1995) Electrostatic dominoes: Long distance propagation of mutational effects in photosynthetic reaction centers of *Rhodobacter capsulatus*, *Biochemistry 34*, 8390−8397.
76. Li, J., Gilroy, D., Tiede, D. M., and Gunner, M. R. (1998) Kinetic phases in the electron transfer from $P^+Q_A^-Q_B$ to $P^+Q_AQ_B^-$ and the associated processes in *Rhodobacter sphaeroides* reaction centers, *Biochemistry 37*, 2818−2829.
77. Remy, A., and Klaus, G (2003) Coupling of light-induced electron transfer to proton uptake in photosynthesis, *Nat. Struct. Biol. 10*, 637−644.
78. Yeates, T. O., Komiya, H., Rees, D. C., Allen, J. P., and Feher, G. (1987) Structure of the reaction center from *Rhodobacter sphaeroides* R-26: Membrane-protein interaction, *Proc. Natl. Acad. Sci. U.S.A. 84*, 6438−6442.
79. Graige, M. S., Paddock, M. L., Feher, G., and Okamura, M. Y. (1999) Observation of the protonated semiquinone intermediate in isolated reaction centers from *Rhodobacter sphaeroides*: Implications for the mechanism of electron and proton transfer in proteins, *Biochemistry 38*, 11465−11473.
80. Katona, G., Andreasson, U., Landau, E. M., Andreasson, L. E., and Neutze, R. (2003) Lipidic cubic phase crystal structure of the photosynthetic reaction centre from *Rhodobacter sphaeroides* at 2.35 angstrom resolution, *J. Mol. Biol. 331*, 681−692.
81. Yosikawa, S., Shinzawa-Itoh, K., and Tsukihara, T. (1998) Crystal structure of bovine heart cytochrome *c* oxidase at 2.8 Å resolution, *J. Bioenerg. Biomembr. 30*, 7−14.
82. Domonkos, I., Malec, P., Sallai, A., Kovács, L., Itoh, K., Shen, G., Ughy, B., Bogos, B., Sakurai, B., Strzalka, K., Wada, H., Itoh, S., Farkas, T., and Gombos, Z., (2004) Phosphatidylglycerol is essential for oligomerization of photosystem I reaction center, *Plant Physiol. 134*, 1471−1478.
83. Kruse, O., Hankamer, B., Konczak, C., Gerle, C., Morris, E., Radunz, A., Schmid, G. H., and Barber, J. (2000) Phosphatidylglycerol is involved in the dimerization of photosystem II, *J. Biol. Chem. 275*, 6509−6514.
84. Ferreira, K. N., Iverson, T. M., Maghlaoui, K., Barber, J., and Iwata, S. (2004) Architecture of the photosynthetic oxygen-evolving center, *Science 303*, 1831−1838.

BI0489356